Polymer Journal (2015) 47, 294–301

www.nature.com/pj

ORIGINAL ARTICLE

The effect of flexible chains on the orientation dynamics of small molecules dispersed in polymer films during stretching

Shogo Nobukawa[1], Yoshihiko Aoki[1], Yoshiharu Fukui[1], Ayumi Kiyama[1], Hiroshi Yoshimura[2], Yutaka Tachikawa[3] and Masayuki Yamaguchi[1]

The effect of flexible chains on the orientation dynamics of small additive molecules in cellulose acetate propionate (CAP) films is investigated during stretching using birefringence and polarized Fourier-transform infrared (FT-IR) spectra measurements. The orientation birefringence is enhanced by additives such as ethylene 2,6-naphthalate (C_2Np) and hexamethylene 2,6-naphthalate (C_6Np) oligomers, suggesting that the additives orient parallel to the CAP chain as a result of an intermolecular orientation correlation referred to as the nematic interaction (NI). At a high drawing temperature, the orientation of C_2Np is stronger than that of C_6Np, indicating that the flexible alkyl chain has reduced the intermolecular NI with CAP. By contrast, C_6Np orients along the stretching direction at low temperatures. Polarized FT-IR spectra show that the orientation of the rigid portions of C_6Np is delayed relative to those of the flexible groups and the matrix CAP chain. Consequently, the contribution of C_6Np to birefringence and its wavelength dependence become stronger as the draw ratios increase.
Polymer Journal (2015) **47,** 294–301; doi:10.1038/pj.2014.126; published online 24 December 2014

INTRODUCTION

The orientation dynamics of polymer chains are strongly related to various polymer properties, including mechanical, optical, thermal and dielectric properties.[1–5] In particular, chain orientation generates an optical anisotropy, namely, birefringence, which is important in optical applications, such as liquid crystal displays, electro-luminescence displays and optical pick-up lenses. To improve the performance of these devices, both the birefringence value and its wavelength dependence must be controlled. For example, quarter-wave plates, one of the most important types of optical film, require a retardation of a quarter of a wavelength for the wide range of visible lights. However, in general, such optical properties cannot be obtained in a conventional film using a single-polymer component.

When polymer films are stretched beyond their glass transition temperature (T_g), orientation birefringence, Δn, is induced. Δn is defined as the difference between the two refractive indices in the directions parallel and perpendicular to the stretching direction, i.e., $n_{||}$ and $n_{\perp}$, respectively, $\Delta n = n_{||} - n_{\perp}$. The orientation birefringence Δn is proportional to the degree of the chain orientation, F, as follows:[6]

$$\Delta n(\lambda) = \Delta n^0(\lambda) F \tag{1}$$

Here, Δn^0 is an intrinsic birefringence where the anisotropic molecule perfectly orients along the stretching direction. As represented in equation 1, Δn^0 is dependent on the wavelength, λ, whereas F is independent of wavelength. Therefore, for single-component polymer films, the wavelength dependence of Δn, $\Delta n(\lambda)/\Delta n(\lambda_0)$, cannot be changed by the chain orientation, as represented by:

$$\frac{\Delta n(\lambda)}{\Delta n(\lambda_0)} = \frac{\Delta n^0(\lambda)}{\Delta n^0(\lambda_0)} = const. \tag{2}$$

To control the birefringence and its wavelength dependence in optical films, a combination of double or multi components with different wavelength dependence is ideal. Various techniques, such as blending with other polymers[7,8] or small molecules,[9–12] copolymerization[13–15] and sheet piling,[16] have been considered. Blending with small molecules is easier and more suitable than other methods for use in industrial applications. For polymer blending and copolymerization, the number of combinations of materials is limited by the poor miscibility of polymer pairs. For lamination, the thermal expansion mismatch between polymer sheets restricts the available temperature range.

The orientation birefringence of the blend, $\Delta n_{\mathrm{blend}}$, is expressed by a simple addition rule given by:

$$\Delta n_{blend}(\lambda) = \sum \Delta n_i(\lambda) = \sum \phi_i \Delta n_i^0(\lambda) F_i \tag{3}$$

where ϕ_i, Δn_i^0 and F_i are the volume fraction, intrinsic birefringence and orientation function, respectively, for component i. As shown in Figure 1, the blend birefringence and its wavelength dependence are determined by the component birefringences. In particular, the concentration and the orientation function of the components

[1]Japan Advanced Institute of Science and Technology, Ishikawa, Japan; [2]DIC Corporation, Chiba Plant, Chiba, Japan and [3]DIC Corporation, Central Research Laboratories, Chiba, Japan
Correspondence: Dr S Nobukawa, School of Materials Science, Japan Advanced Institute of Science and Technology, 1-1 Asahidai, Nomi, Ishikawa 923-1292, Japan.
E-mail: nobukawa@jaist.ac.jp
Received 2 October 2014; revised 4 November 2014; accepted 6 November 2014; published online 24 December 2014

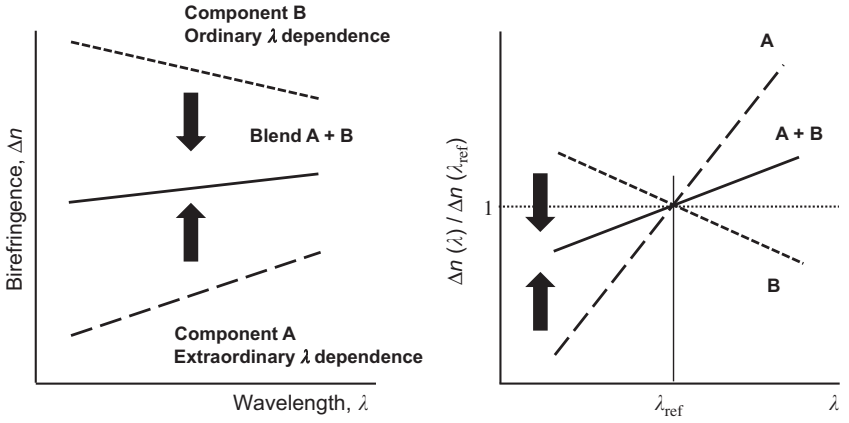

Figure 1 Schematic representation of the ability to control birefringence and its wavelength dependence by mixing additives with a matrix polymer.

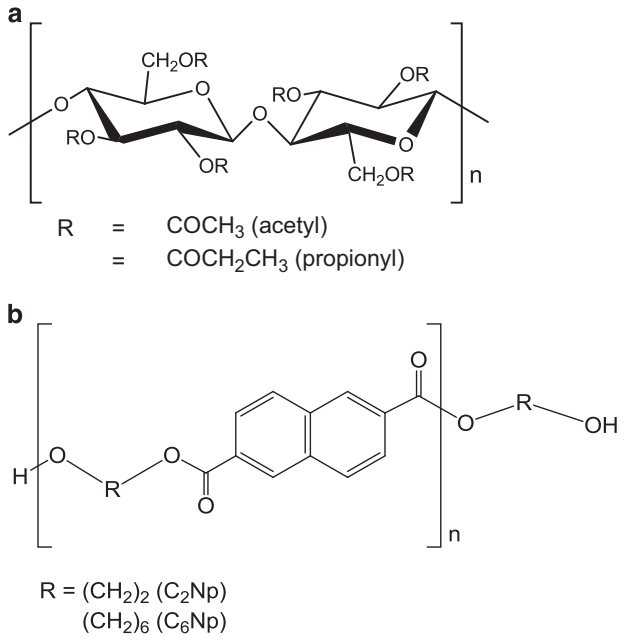

Figure 2 Chemical structures of (**a**) CAP and (**b**) additives.

contribute to the birefringence, as shown in equation 3. Small molecules reduce the thermal resistance of polymer films via the plasticization effect, thereby limiting the additive content. By contrast, the additive orientation is determined by an intermolecular orientation correlation, the nematic interaction (NI).[17,18] The orientation function of additives, F_{add}, is proportional to that of matrix polymers, F_{poly}, suggesting that the wavelength dependence cannot be controlled by the stretching conditions if the additive orientation dynamics are completely coupled to those of the matrix polymer chains. However, if the additive orientation is independently generated from the matrix polymer, the wavelength dependence can be modified for blend films with the same composition.

Choudhury *et al.*[19] investigated the orientation dynamics of high-molecular weight poly(ethylene terephthalate) (PET) using ^{1}H-^{13}C cross-polarization magic-angle-spinning (CP/MAS) NMR spectroscopy. According to their results, the ethylene in PET exhibits 10 times shorter relaxation times than the phenyl ring, indicating that the orientation of the flexible chain is induced by stretching before the orientation of the rigid portions of the polymer. Therefore, for small molecules with similar structures to PET, the flexible and rigid portions may exhibit different orientation times in polymer films during stretching, allowing for the control of wavelength dependence of birefringence.

In this study, the effect of alkyl chains on the orientation dynamics of small additives in polymer films during stretching is investigated. Two types of alkyl naphthalates are used as model compounds and are mixed with cellulose acetate propionate (CAP), which is used as a model polymer for optical films.[20] In particular, the additive orientations in CAP films are investigated using birefringence measurements and Fourier-transform infrared (FT-IR) spectroscopy.

Table 1 Molecular weight (M_n), degree of polymerization (DP), melting point (T_m) and intrinsic birefringence (Δn^0) of additives

Additive	M_n[a]	DP	T_m/°C[b]	Δn^{0}[c]
C_2Np	390	1.3	85	0.14
C_6Np	643	1.6	97	0.081

[a]Estimated by a method of end-group determination using potassium hydrate.
[b]Determined by DSC.
[c]Calculated by a molecular dynamics simulation with bond-polarizability parameter.[21]

EXPERIMENTAL PROCEDURE

Samples

CAP (Figure 2) was produced by Eastman Chemical Company (TN, USA). The weight-average and number-average molecular weights (M_w and M_n) of CAP were 2.1×10^5 and 7.7×10^4, respectively, as determined by gel-permeation chromatography (GPC; HLC-8020 TOSOH, Tokyo, Japan) with a polystyrene standard. Degrees of substitution for acetyl and propionyl groups per pyranose unit of CAP were 0.19 and 2.58, respectively. Ethylene 2,6-naphthalate and hexamethylene 2,6-naphthalate oligomers (C_2Np and C_6Np, Figure 2) were used as additives and were synthesized from alkane diol and dimethyl naphthalene 2,6-dicarboxylate (DMNDC). In brief, DMNDC and ethylene glycol (EG) (or 1,6-hexamethylene diol (HD)) with an excess molar quantity relative to DMNDC were mixed in a flask. After tetraisopropyl titanate was added as a catalyst for the esterification reaction, the mixture was stirred at 200 °C for 12 h under a nitrogen atmosphere. The residual EG (or HD) was then removed at 200 °C *in vacuo* to obtain C_2Np or C_6Np. M_n was calculated from the fraction of hydroxyl groups at the chain end in a molecule, which was estimated using a method of end-group determination with potassium hydrate. The melting temperatures (T_ms) of the additives were evaluated by a differential scanning calorimetry (DSC-822e, Mettler Tolede, Greifensee, Switzerland). The values of M_n and T_m are summarized in Table 1. As shown in the table, the

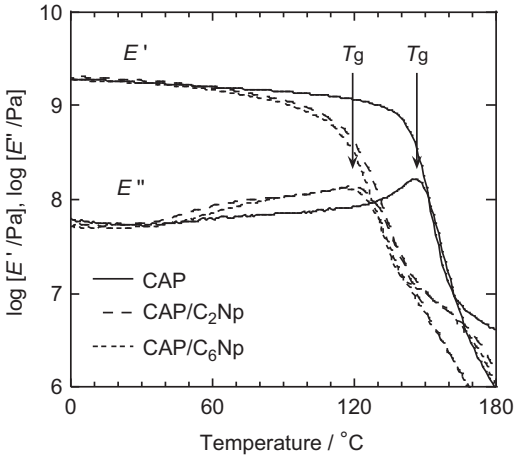

Figure 3 Temperature dependence of tensile storage and loss moduli (E' and E'') for bulk CAP and CAP/additive (100/10 wt/wt) films. The oscillatory frequency is 10 Hz and the heating rate is 2 °C min^{-1}.

degrees of polymerization of C_2Np and C_6Np are slightly different (1.3 and 1.6, respectively).

Blends of CAP and C_2Np (or C_6Np) at a weight ratio of 100/10 were prepared using a 60 cc batch-type internal mixer (Labo-plastmil, Toyoseiki, Japan) at 200 °C for 6 min with the blade rotation speed of 30 rpm. The preparation conditions were determined as described in our previous work.[21] To avoid chemical reactions, such as hydrolysis degradation and transesterification, CAP was dried *in vacuo* at 80 °C for 2 h before melt-mixing. After being kept in a vacuum oven at room temperature for at least 24 h, the blend samples were compressed into sheets with a thickness of 20–30 μm at 200 °C for 5 min under 10 MPa using a compression-molding machine (Table-type-test press SA-303-I-S, Tester Sangyo, Saitama, Japan) and were subsequently cooled to 25 °C for 5 min.

Measurements

Dynamic mechanical analysis (DMA) of the sample films was carried out using a tensile oscillatory rheometer (DVE-E4000, UBM, Kyoto, Japan) to determine tensile storage and loss moduli (E' and E'', respectively) at 10 Hz as a function of temperature from 25 to 180 °C with a heating rate of 2 °C min^{-1}.

DSC was utilized to evaluate the crystallinity of CAP and CAP/additive films during heating with a heating rate of 10 °C min^{-1}.

A hot-stretching test on the films was carried out with a strain rate of 0.05 s^{-1} using a tensile drawing machine (DVE-3, UBM, Japan). The stretching temperatures were determined from the DMA data, at the points at which the tensile modulus was 10 or 100 MPa at 10 Hz. The films were immediately quenched by cold air blowing after stretching to avoid relaxation of molecular orientation.

The stretched films were kept in a humidified chamber (IG420, Yamato, Japan) at 25 °C and 50% RH for 24 h to prevent previously reported moisture effects on birefringence data.[22] During the stock process in the chamber, the chain orientation of CAP does not relax, because its glass transition temperature (T_g) is much higher than the storage temperature, even with the additive blends. The birefringence of the drawn films was measured as a function of wavelength using an optical birefringence analyzer (KOBRA-WPR, Oji Scientific Instruments, Hyogo, Japan).[23]

To evaluate orientation functions (F) for CAP, C_2Np and C_6Np in the stretched films, polarized FT-IR spectra were measured over the wavelength range of 400–4000 cm^{-1} with a resolution of 4 cm^{-1} at room temperature using an FT-IR spectrometer (Jasco, Tokyo, Japan) equipped with a wire-grid polarizer. The details of the measurement for molecular orientation are explained in the supplementary information.

Table 2 Glass transition temperature (T_g) and drawing temperature (T_{draw}) for CAP and CAP/additive blends

		T_{draw}/°C[b] ($T_{draw}-T_g$)	
	T_g/°C[a]	E' = 10 MPa	E' = 100 MPa
CAP	146	163 (+17)	152 (+6)
CAP/C_2Np	119	146 (+27)	127 (+8)
CAP/C_6Np	116	149 (+33)	133 (+17)

[a]Defined as a peak temperature of E'' in Figure 3.
[b]Determined as a temperature where E' is 10 or 100 MPa.

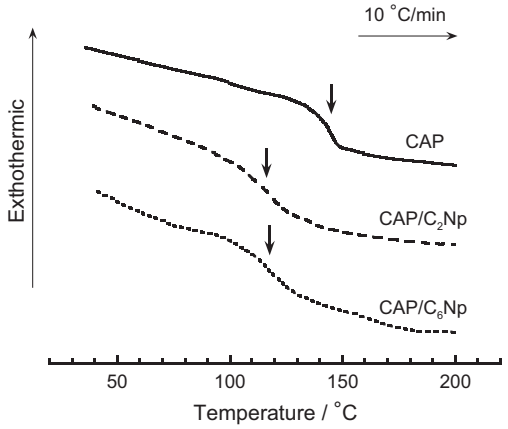

Figure 4 DSC curves of CAP and CAP/additive films during heating with a heating rate of 10 °C min^{-1}. The arrows indicate the glass transition temperatures.

RESULTS AND DISCUSSION

Miscibility and plasticization of CAP with additives

Figure 3 shows the dynamic mechanical properties of CAP and CAP/additive blends in the temperature range of 0 to 180 °C. The glass transition temperature (T_g) is defined as the peak temperature of the loss modulus, E'', and was determined to be 146, 119 and 116 °C for bulk CAP, CAP/C_2Np and CAP/C_6Np, respectively, Table 2. Both blends demonstrated broader glass transitions relative to bulk CAP, indicating that the relaxation time distribution for the glass transition becomes wider with the addition of C_2Np and C_6Np. This phenomenon, which can be explained by the concentration fluctuation theory, has been reported in many polymer blends, including plasticized polymers.[24–26] The concentration distributions in the systems are related to the broadness of the glass transition. Furthermore, the reductions in the T_g of CAP by the addition of C_2Np and C_6Np are similar, which may be due to their similar chemical structures and molecular weights, as shown in Figure 2 and Table 1.

In the rubbery region above T_g, CAP/additive blends demonstrate a similar storage modulus, E', (~10 MPa) to that of bulk CAP. In general, the rubbery plateau modulus for crystalline polymers, such as cellulose acetate, is 100 MPa.[27,28] However, as shown in Figure 4, DSC curves for the films do not show a melting peak, which could appear between 150 and 200 °C for CAP.[23] This result suggests that the crystalline content is negligibly small for CAP in both bulk and blend films.

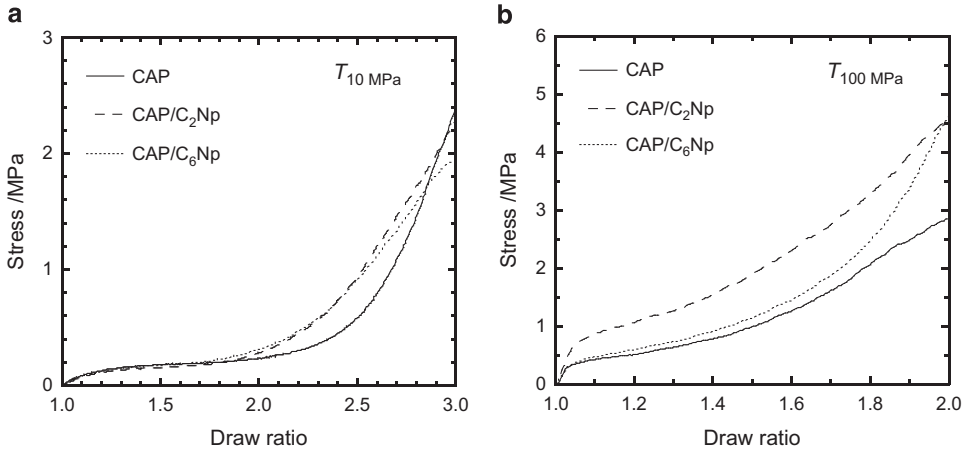

Figure 5 Stress–strain curves of CAP and CAP/additive films at two draw temperatures where E' is (**a**) 10 or (**b**) 100 MPa. The strain rate is $0.05\,s^{-1}$.

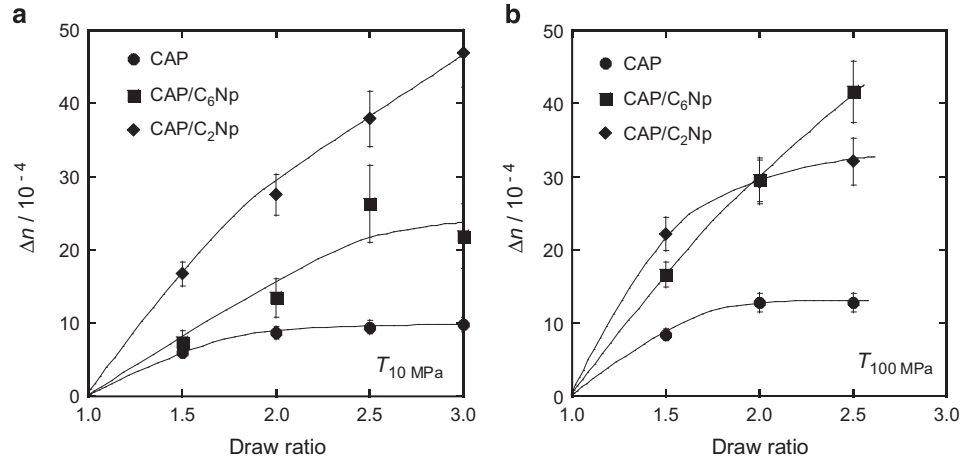

Figure 6 Orientation birefringence, Δn, of CAP and CAP/additive (100/10 wt/wt) films stretched with various draw ratios at (**a**) $T_{10\,MPa}$ and (**b**) $T_{100\,MPa}$.

Stress–strain behavior of CAP and CAP/additive films

Stretching polymer films induces chain orientation, which contributes to tensile stress, σ, and birefringence, Δn. According to the stress-optical rule, the following relation between Δn and σ is obtained:

$$\Delta n = C\sigma \tag{4}$$

Considering equation 1, σ is proportional to the orientation function, F, and to Δn, that is, the chain orientation can be controlled by altering the stress level.

Before stretching CAP and CAP/additive films, two drawing temperatures (T_{draw}s) were determined from the storage modulus in Figure 3 according to our previous work.[20] As shown in Table 2, the gap between T_{draw} and T_g increases with additives, because the glass transition is broadened (Figures 3 and 4). Figure 5 shows the stress–strain (S–S) curves of CAP and CAP/additive films at two T_{draw}s ($T_{10\,MPa}$ or $T_{100\,MPa}$). For CAP films, the stress levels are very different between $T_{10\,MPa}$ and $T_{100\,MPa}$. However, the orientation function of CAP is similar for the two draw temperatures and is dependent on the draw ratio. Thus, the orientation behavior of CAP chains is insensitive to temperature under the experimental conditions of this study. This result may be because the tensile stress at the lower temperature ($T_{100\,MPa}$) includes the glassy stress related to the local distortion in CAP chains and the rubbery stress that originates from the chain orientation, as reported by Maeda and Inoue.[29] Consequently, the rubbery stress is similar at the two draw temperatures, indicating that the difference in the orientation function of CAP is small.

By comparing the S–S curves in Figure 5, it can be seen that the three films exhibit the same level of tensile stress at $T_{10\,MPa}$. By contrast, at $T_{100\,MPa}$, the stress value for CAP/C_2Np is slightly larger than the stress values for CAP and CAP/C_6Np. However, the similar rubbery stresses indicate that the orientation function of CAP is similar in bulk and blend films. The same level of orientation function suggests that the orientation birefringence of CAP is similar between the bulk and the blend. Therefore, the difference in orientation birefringence between CAP and CAP/additives originates from the additive orientation, as previously discussed.[20]

Orientation birefringence of stretched CAP/additive films

Figure 6 shows the orientation birefringence, Δn, of CAP and CAP/additive films stretched at two drawing temperatures. As shown in Figure 5, Δn values of all samples monotonically increase with the draw ratio and the tensile stress, σ. Comparing Figures 5 and 6 shows that the curves of Δn versus draw ratio are clearly different from those of σ for both bulk and blend materials. In general, both σ and Δn of amorphous polymers at the rubbery state originate from the chain orientation; therefore, the curves of these properties versus the draw ratio should be the same, as predicted by equation 4. By contrast, according to Yamaguchi *et al.*,[23] Δn for CAP is generated by the

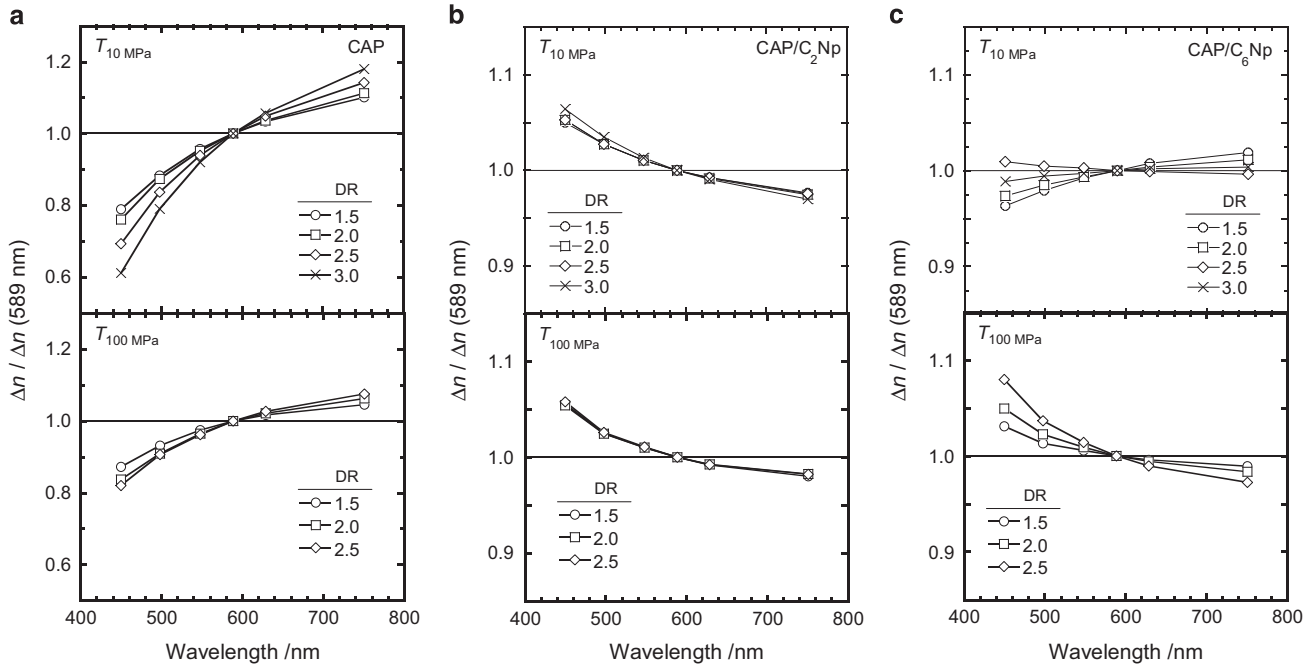

Figure 7 Comparison of wavelength dependence for Δn of (**a**) CAP, (**b**) CAP/C_2Np, and (**c**) CAP/C_6Np films stretched with various draw ratios at two drawing temperatures.

alignment of substitution groups, acetyl and propionyl groups, because the polarizability anisotropy of a pyranose ring in the main chain is negligibly small. Furthermore, the alignments of acetyl and propionyl groups are not completely cooperative with the main chain orientation at higher draw ratios; thus, the curves of σ and Δn versus draw ratio were different for CAP and CAP/additive blends, as shown in Figures 5 and 6.

In Figure 6, the Δn values of CAP/additive films are larger than that of the CAP film, demonstrating that the additive molecules contribute to Δn, as represented by equation 3. As shown in Figure 6a, the effect of C_2Np is larger than that of C_6Np for Δn at $T_{10\,MPa}$. However, the data in Figure 6b indicate that the effects of C_6Np and C_2Np are more similar at $T_{100\,MPa}$. This result demonstrates that the contribution of the additives to Δn depends on the drawing temperature. As reported in our previous papers,[20,21] the enhancement of birefringence is generated by the additive orientation, which is induced by the chain orientation of surrounding polymers, that is, the intermolecular NI. Therefore, the effect of the drawing temperature on the orientations of C_2Np and C_6Np in CAP can be compared.

Figure 7 compares the wavelength dependence of Δn for CAP and CAP/additive films stretched at various draw ratios. As reported by Yamaguchi *et al.*,[23] CAP films demonstrate extraordinary wavelength dispersion, in which Δn increases with wavelength, and the slope of the curve increases with the draw ratio. However, CAP/additive films, with the exception of CAP/C_6Np at $T_{10\,MPa}$, exhibit normal wavelength dispersion, where Δn decreases with wavelength. Furthermore, the wavelength dependence is affected by the additive species. In the case of the CAP/C_2Np film, the wavelength dependence of Δn is independent of the draw ratio. By contrast, for the CAP/C_6Np film, the wavelength dependence changes gradually from extraordinary to ordinary with increasing draw ratio, suggesting that the additive orientation is slower than the chain orientation of CAP during stretching.

According to equations 2 and 3, the wavelength dependence of Δn in binary blend films is determined by the ratio of two components. As the wavelength dependence of CAP increases with the draw ratio, the lack of change in wavelength dependence of CAP/C_2Np (Figure 7b) suggests that the C_2Np contribution to birefringence is more greatly enhanced at increased draw ratios. In addition, the wavelength dispersion of CAP/C_6Np was changed from extraordinary to ordinary at large draw ratios, indicating that the contribution of C_6Np increases during stretching, similarly to the case of CAP/C_2Np. These results may be related to the observed differences in time/strain required for the orientation of CAP chains and additives, as orientation is temperature dependent. To analyze the orientation dynamics of C_2Np and C_6Np in CAP films at two drawing temperatures, molecular orientation is assessed using polarized FT-IR spectra in the following sections.

Molecular orientation of CAP and additives in stretched films

Polarized FT-IR spectroscopy can provide the orientation function, F, of CAP and additives in stretched films by the following equation:

$$F = \frac{R_0 + 1}{R_0 - 2}\,\frac{R - 1}{R + 2} \tag{5}$$

Here, R is a ratio of peak intensities, $A_{\parallel}/A_{\perp}$. The subscripts of peak absorbance, A, represent measurements made parallel and perpendicular to the stretching direction axis. $R_0 = 2\cot^2\beta$, where β is the angle between the transition moment corresponding to the absorption band and the chain axis. The orientation function of CAP, F_{CAP}, was evaluated using the peaks at 806 and 884 cm^{-1}. Orientations of the aromatic portions in C_2Np and C_6Np were investigated using the peak at 772 cm^{-1}. The orientation function of the hexyl chain in C_6Np was also estimated from the peak at 2860 cm^{-1}. The ethylene chain orientation of C_2Np cannot be evaluated, because the peak of the C-H stretching mode appears at the same wavenumber as that of CAP. Analysis of the F values is described in the supplementary information.

Figure 8a shows the orientation function of CAP, F_{884}, which was calculated from the peak at 884 cm^{-1}. The degree of chain orientation, F_{884}, monotonically increases with the draw ratio, corresponding

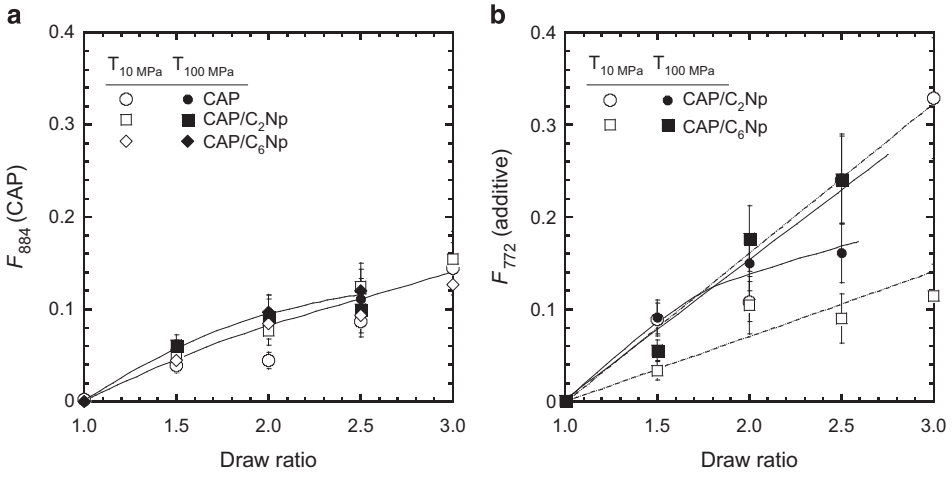

Figure 8 Orientation functions for (**a**) CAP and (**b**) additives in stretched films with various draw ratios at two drawing temperatures.

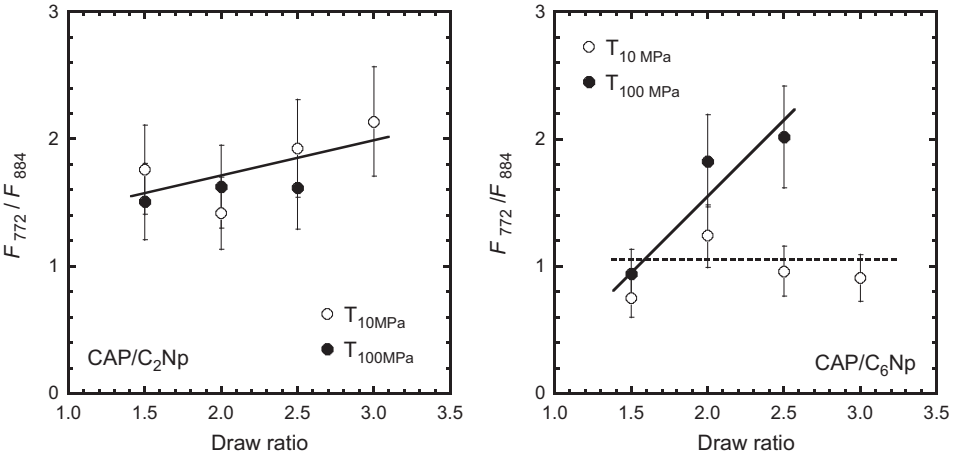

Figure 9 Ratio of orientation functions for additive and CAP in blend films stretched with various draw ratios at two drawing temperatures.

to the stress–strain curve in Figure 5. This phenomenon is because the tensile stress originates from the chain orientation, as mentioned previously. Figure 8a indicates the same level of CAP chain orientation in both the bulk and the blends, although the degrees of orientation differ slightly between $T_{10\,MPa}$ and $T_{100\,MPa}$.

Figure 8b shows the relationship between the draw ratio and orientation function at 772 cm^{-1}, F_{772}, which represents the orientation of the aromatic groups in C_2Np and C_6Np. The orientation of C_2Np is stronger than that of C_6Np at $T_{10\,MPa}$, while it is slightly weaker at $T_{100\,MPa}$. The differences in F_{772} for C_2Np and C_6Np at the two temperatures correspond to the birefringence results in Figure 6. As mentioned before, additive orientation (F_{add}) is induced by the chain orientation of the surrounding polymer (F_{poly}) via NI,[18] as represented by the following equation:

$$F_{add} = \left[\frac{\phi_{poly}\varepsilon_{poly,add}}{1-\phi_{poly}\varepsilon_{poly,poly}}\right]F_{poly} \quad (6)$$

Here, ϕ is a volume fraction and $\varepsilon_{i,j}$ is the NI parameter between components i and j. As ϕ_{poly} and $\varepsilon_{poly,poly}$ are constants for the samples in this study, the degree of additive orientation F_{add} ($=F_{722}$) is determined by only the intermolecular NI represented by $\varepsilon_{poly,add}$. Therefore, the additive orientation due to the NI can be assessed using the ratio F_{add}/F_{poly} ($=F_{772}/F_{884}$).

Orientation dynamics of C_2Np and C_6Np induced by NI

Before investigation of the orientation dynamics of the additives in CAP, the effect of molecular weight should be noted. In our previous work,[20] the effect of molecular weight on the orientation of alkyl terephthalate oligomers in CAP was discussed. According to that work, for degrees of polymerization (DP) greater than 2, the orientation function of the additive oligomers increases with increasing DP. However, for lower DP values (1 or 2), the additive orientation is more similar. According to these results, in the current study, the low DP values of C_2Np and C_6Np (1.3 and 1.6, respectively) indicate that the effects of DP on the orientation dynamics can be ignored.

To discuss the orientation dynamics of C_2Np and C_6Np in CAP during stretching, F_{772}/F_{884} was calculated at various draw ratios, as shown in Figure 9. The ratios for CAP/C_2Np exhibit the same dependence on the draw ratio at $T_{10\,MPa}$ and $T_{100\,MPa}$ and slightly increase with the draw ratio. This result suggests that the C_2Np orientation is simply generated by the intermolecular NI with the chain orientation of CAP. However, F_{772}/F_{884} for CAP/C_6Np is clearly dependent on the drawing temperature. The ratio F_{772}/F_{884} at $T_{100\,MPa}$ is larger than that at $T_{10\,MPa}$ at high draw ratios, resulting in the

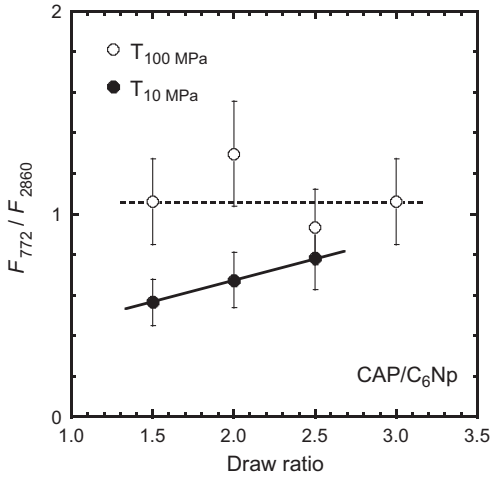

Figure 10 Ratio of orientation functions for rigid and flexible portions of C_6Np in blend films stretched with various draw ratios.

difference in the effects of C_6Np at the two draw temperatures shown in Figure 6. In addition, the ratio at $T_{100\,MPa}$ increases with the draw ratio, indicating that the orientation of the aromatic group in C_6Np, which corresponds to the FT-IR peak at 772 cm^{-1}, is delayed relative to the chain orientation of CAP at $T_{100\,MPa}$.

Choudhury *et al.*[19] investigated chain dynamics of high-molecular weight poly(ethylene terephthalate) (PET) using ^1H-^{13}C cross-polarization magic-angle-spinning (CP/MAS) NMR spectroscopy. They explained that the relaxation time of the phenyl ring in PET is 10 times longer than that of the ethylene group, suggesting that the rigid and flexible portions have different time/strain requirements for orientation. As the additive molecules in this study have similar structures to PET, the above result is applicable for the discussion of orientation dynamics in this study.

The orientation of the flexible portion in C_2Np cannot be investigated, because its FT-IR peak (C-H stretching band) overlaps with that of CAP. However, the flexible hexa-methylene group orientation in C_6Np can be evaluated, as the peak is located at a different wavenumber from that of the matrix polymer. The orientation functions of the rigid and flexible portions in C_6Np, which are estimated from FT-IR peaks at 772 and 2860 cm^{-1}, respectively, are shown in Figure 10. At a higher drawing temperature ($T_{10\,MPa}$), F_{772} and F_{2860} are comparable, indicating that the flexible and rigid portions in C_6Np have the same orientation time in the stretched CAP film. However, at a lower temperature ($T_{100\,MPa}$), F_{772} becomes closer to F_{2860} with increasing draw ratio, implying that the aromatic group in the C_6Np molecule has a longer relaxation time than the alkyl chain. This orientation behavior of C_6Np corresponds to the chain dynamics of PET reported by Choudhury *et al.*

As shown in Figure 9, the orientation of C_6Np at a low temperature ($T_{100\,MPa}$) was stronger than that at a high temperature ($T_{10\,MPa}$). This phenomenon was also reported for other types of additives in our previous work.[20] According to the NI theory, additive orientation is induced by the chain orientation of matrix polymers due to the intermolecular NI, that is, orientation coupling. Therefore, additive orientation (F_{add}) should be cooperative with or delayed from the matrix polymer chain orientation (F_{poly}). Thus, the ratio of orientation functions F_{add}/F_{poly} decreases at lower temperatures, as the additive relaxation time increases. However, at low temperatures, the glassy stress generates local chain distortion of polymers, which could enhance flexible chain alignment, such as the *trans* formation of polyethylene chains. In the experimental data, the orientation of the flexible portion (hexa-methylene group) of C_6Np at $T_{100\,MPa}$ is stronger than that at $T_{10\,MPa}$. For C_2Np, the flexible portion is too short to induce orientation at $T_{100\,MPa}$. The alignment of the flexible portions enhances the orientation of rigid portions in C_6Np, especially at $T_{100\,MPa}$, as shown in Figure 9.

On the basis of the above discussion, the following model is considered to explain the orientation dynamics of C_6Np in CAP films. First, the chain orientation of CAP induces the alignment of flexible portions in C_6Np. At low temperatures near the T_g, the local chain distortion that originates from the glassy stress also generates flexible chain orientation. Second, the rigid (aromatic) portion orients after the flexible portion orientation due to the difference in orientation relaxation times. As a result, the wavelength dependence of birefringence for CAP/C_6Np changes during stretching, as shown in Figure 7c. In general, the wavelength dependence of orientation birefringence of optical polymers is difficult to control by processing conditions. However, as discussed in this study, the wavelength dependence in polymer blends can be modified by adjusting the drawing conditions for the orientation dynamics of additive molecules.

CONCLUSIONS

To control the wavelength dependence of orientation birefringence for CAP film, we investigated the orientations of small additive molecules in CAP films during stretching. To examine the effect of flexible chains on the orientation dynamics, two types of oligomeric additives, 2,6-ethylene naphthalate (C_2Np) and 2,6-hexamethyl naphthalate (C_6Np), were used in this study.

The birefringence of the CAP/additive film was larger than that of the pure CAP film, indicating that the additive orientation is generated by an orientation correlation represented by an intermolecular NI. Furthermore, C_2Np demonstrated improved birefringence of CAP relative to C_6Np at higher drawing temperatures. However, at lower temperatures, C_6Np showed stronger enhancement of birefringence than C_2Np. This result suggests that the orientation of C_6Np is promoted at lower temperatures more than that of C_2Np. The wavelength dependence of birefringence of CAP/C_6Np films was gradually changed from extraordinary to ordinary, indicating that the orientation dynamics of C_6Np are not cooperative with the chain orientation of CAP, despite the orientation being induced by NI.

From polarized FT-IR spectra, the orientation functions of CAP, C_2Np and C_6Np were evaluated. For C_6Np, orientations of the hexa-methylene group and the aromatic ring were not coupled during stretching at lower temperatures. This result suggests that the flexible portion of C_6Np oriented before the alignment of the rigid portion, that is, the flexible and rigid portions in alkyl naphthalate molecules have different orientation times. By applying this phenomenon, birefringence and its wavelength dependence in polymer films containing additives could be controlled.

ACKNOWLEDGEMENTS

This work was partially supported by a Grant-in-Aid for Young Scientists B (25870268) and by a grant from the Kyoto Technoscience Center in 2013.

1 McCrum, N. G., Read, B. E. & Williams, G. *Anelastic and Dielectric Effects in Polymeric Solids* (Dover Publications, New York, USA, 1967).
2 Doi, M. & Edwards, S. F. *The Theory of Polymer Dynamics* (Oxford University Press, New York, USA, 1986).
3 Harding, G. F. *Optical Properties of Polymers* (ed. Meeten G. H.) (Elsevier Applied Science Publishers, London, UK, 1986).

4 Korus, J., Hempel, E., Beiner, M., Kahle, S. & Donth, E. Temperature dependence of alpha glass transition cooperativity. *Acta Polym.* **48**, 369–378 (1997).
5 Taniguchi, N., Urakawa, O. & Adachi, K. Calorimetric study of dynamical heterogeneity in toluene solutions of polystyrene. *Macromolecules* **37**, 7832–7838 (2004).
6 Ward, I. M. The measurement of molecular orientation in polymers by spectroscopic techniques. *J. Poly. Sci. Part C Poly. Sym.* **58**, 1–21 (1977).
7 Saito, H. & Inoue, T. Chain orientation and instrinsic anisotropy in birefringence-free polymer blends. *J. Poly. Sci. Part-B Poly. Phys.* **25**, 1629–1636 (1987).
8 Uchiyama, A. & Yatabe, T. Analysis of extraordinary birefringence dispersion of uniaxially oriented poly(2,6-dimethyl 1,4-phenylene oxide)/atactic polystyrene blend films. *Japan J. App. Phys. Part-1* **42**, 3503–3507 (2003).
9 Tagaya, A., Iwata, S., Kawanami, E., Tsukahara, H. & Koike, Y. Zero-birefringence polymer by the anisotropic molecule dope method. *App. Opt.* **40**, 3677–3683 (2001).
10 Tagaya, A., Ohkita, H., Harada, T., Ishibashi, K. & Koike, Y. Zero-birefringence optical polymers. *Macromolecules* **39**, 3019–3023 (2006).
11 Abd Manaf, M. E., Tsuji, M., Shiroyama, Y. & Yamaguchi, M. Wavelength dispersion of orientation birefringence for cellulose esters containing tricresyl phosphate. *Macromolecules* **44**, 3942–3949 (2011).
12 Abd Manaf, M. E., Miyagawa, A., Nobukawa, S., Aoki, Y. & Yamaguchi, M. Incorporation of low-mass compound to alter the orientation birefringence in cellulose acetate propionate. *Opt. Mater.* **35**, 1443–1448 (2013).
13 Iwasaki, S., Satoh, Z., Shafiee, H., Tagaya, A. & Koike, Y. Design and synthesis of zero-zero-birefringence polymers in a quaternary copolymerization system. *Polymer* **53**, 3287–3296 (2012).
14 Uchiyama, A., Ono, Y., Ikeda, Y., Shuto, H. & Yahata, K. Copolycarbonate optical films developed using birefringence dispersion control. *Polym. J.* **44**, 995–1008 (2012).
15 Cimrova, V., Neher, D., Kostromine, S. & Bieringer, T. Optical anisotropy in films of photoaddressable polymers. *Macromolecules* **32**, 8496–8503 (1999).
16 Cho, C. K., Kim, J. D., Cho, K., Park, C. E., Lee, S. W. & Ree, M. Effects of the lamination temperature on the properties of poly(ethylene terephthalate-co-isophthalate) in polyester-laminated tin-free steel can - I. Characterization of poly (ethylene terephthalate-co-isophthalate). *J. Adh. Sci. Tech.* **14**, 1131–1143 (2000).
17 Doi, M., Pearson, D., Kornfield, J. & Fuller, G. Effect of nematic interaction in the orientational relaxation of polymer melts. *Macromolecules* **22**, 1488–1490 (1989).
18 Nobukawa, S., Urakawa, O., Shikata, T. & Inoue, T. Evaluation of nematic interaction parameter between polymer segments and low-mass molecules in mixtures. *Macromolecules* **43**, 6099–6105 (2010).
19 Choudhury, R. P., Lee, J. S., Kriegel, R. M., Koros, W. J. & Beckham, H. W. Chain dynamics in antiplasticized and annealed poly(ethylene terephthalate) determined by solid-state NMR and correlated with enhanced barrier properties. *Macromolecules* **45**, 879–887 (2012).
20 Nobukawa, S., Aoki, Y., Yoshimura, H., Tachikawa, Y. & Yamaguchi, M. Effect of aromatic additives with various alkyl groups on orientation birefringence of cellulose acetate propionate. *J. Appl. Polym. Sci.* **130**, 3465–3472 (2013).
21 Nobukawa, S., Hayashi, H., Shimada, H., Kiyama, A., Yoshimura, H., Tachikawa, Y. & Yamaguchi, M. Strong orientation correlation and optical anisotropy in blend of cellulose ester and poly(ethylene 2,6-naphthalate) oligomer. *J. Appl. Polym. Sci.* **131**, 40570 (2014).
22 Abd Manaf, M. E., Tsuji, M., Nobukawa, S. & Yamaguchi, M. Effect of moisture on the orientation birefringence of cellulose esters. *Polymers* **3**, 955–966 (2011).
23 Yamaguchi, M., Okada, K., Abd Manaf, M. E., Shiroyama, Y., Iwasaki, T. & Okamoto, K. Extraordinary wavelength dispersion of orientation birefringence for cellulose esters. *Macromolecules* **42**, 9034–9040 (2009).
24 Hains, P. J. & Williams, G. Molecular motion in polystyrene-plasticizer systems as studied by dielectric relaxation. *Polymer* **16**, 725–729 (1975).
25 Williams, G., Smith, I. K., Aldridge, G. A., Holmes, P. A. & Varma, S. Changes in molecular dynamics during the bulk polymerization of an epoxide/diamine mixture containing inert diluents as studied using dielectric relaxation spectroscopy. *Macromolecules* **34**, 7197–7209 (2001).
26 Lodge, T. P. & McLeish, T. C. B. Self-concentrations and effective glass transition temperatures in polymer blends. *Macromolecules* **33**, 5278–5284 (2000).
27 Kono, H., Numata, Y., Erata, T. & Takai, M. Structural analysis of cellulose triacetate polymorphs by two-dimensional solid-state C-13-C-13 and H-1-C-13 correlation NMR spectroscopies. *Polymer* **45**, 2843–2852 (2004).
28 Yamaguchi, M. *Optical Properties of Cellulose Esters and Their Blends* (eds Lejeune, A., Deprez, T.) (Nova Science Publishers, New York, USA, 2010).
29 Maeda, A. & Inoue, T. On the viscoelastic segment size of cellulose. *Nihon Reoroji Gakkaishi* **39**, 159–163 (2011).

Supplementary Information accompanies the paper on Polymer Journal website (http://www.nature.com/pj)